Proceedings of the 12th International Conference on Fluid Flow, Heat and Mass Transfer (FFHMT 2025)
July 15, 2025 - July 17, 2025 | Imperial College London Conference, London, United Kingdom
Paper No. 144
DOI: 10.11159/ffhmt25.144

Adjoint-Based Shape Optimization Of Fin Geometry Using An Isothermal Streamwise Periodic Flow Solver.

Nitish Anand[1,2]
[1]Vlaams Instelling voor technologish onderzoek (VITO)
Boertang 200, Mol 3600, Belgium
nitish.anand@vito.be
[2]Techniche Universiteit Delft
Kluyverweg 1, Delft 2629HS, The Netherlands.

Abstract – The optimal design of heat exchanges is critical for a wide range of existing and emerging technologies. Traditional design methods often use experimental correlations to estimate thermal and hydraulic performance. However, CFD-based design methods have recently evolved as an alternative to these conventional methods. This paper proposes a CFD-based shape optimization method to design a two-dimensional representation of cylindrical fins. The method consists of a CAD-based parametrization tool and uses a streamwise periodic flow solver to estimate the performance of the fins. In addition, to enable gradient-based optimization, the sensitivity of the objective function with respect to the design variables is provided to the optimizer through an adjoint-based method. The proposed shape optimization method was applied to design cylindrical fins operating at laminar and turbulent flow regimes. The optimization results show that the fluid dynamic performance of the fins increased by 16.5% for the laminar case and 35.8% for the turbulent case while maintaining their thermal performance to their baseline values.

Keywords**:** streamwise periodic flow solver, adjoint-based optimization framework, isothermal walls

1. Introduction

Heat exchangers are vital components in a wide range of existing and emerging technologies. The performance of the heat exchanges often directly translates into the performance of the entire system. Thus, making the design of the heat exchangers extremely critical for all technologies.

Traditionally, the design of heat exchangers is performed using empirical methods like NTU and LMTD. Meanwhile, the hydraulic performance is determined using correlation formulated through extensive experimental campaigns. These methods are widely used in the scientific community, thanks to their simplicity and inexpensive computational demand. However, the accuracy of these methods is limited to only simple geometries and thus cannot be extrapolated to complex geometries possible through novel manufacturing techniques.

As an alternative to these methods, recently, computational fluid dynamic (CFD)-based shape optimization methods have evolved. In this method, CFD is used to estimate the thermo-hydraulic performance of the heat-exchanger geometry and in subsequent steps, the geometry is modified to obtain an optimum design. Recently, the CFD-based shape optimization approach was presented by Ref. [1], wherein the shape of the fins was parametrized using the NURBS curve. The reported framework used a multi-objective gradient-free method to optimize a tube bundle. Similarly, Ref. [2] reports optimization of elliptical tube banks using a multi-objective genetic algorithm. In the context of adjoint-based shape optimization methods, Ref. [3] reports shape optimization framework using FFD boxes and applies the method to optimize the shape of an isolated fin. More recently, Ref. [4] used an adjoint-based shape optimization method to simultaneously optimize the shape and layout of the elliptical fins. In addition, Ref. [5] showcased the concurrent optimization of multiple heat-transfer surfaces using a CAD-based parametrization method coupled with an adjoint-based shape optimization framework.

Although CFD-based methods have proved to be a promising alternative to traditional design methods, it does suffer from high computational costs. This high cost stems from the relatively high number of volume elements required to discretize the intricate heat exchanger geometry. To circumvent this, recently, streamwise periodic flow solvers have been replacing traditional solvers to simulate flow in heat exchangers.

Streamwise periodic (SP) flow solver applies to channels where the area change is periodic in the streamwise direction. Using this periodic change in the area, a periodic definition of flow properties like, velocity, pressure and temperature can be formulated. Applying these periodic formulations to standard Navier-Stokes (NS) equations gives us additional source terms which constitute to SP flow solver. Thanks to the SP flow solver, heat-exchanger geometries with repeating fin structures can be simulated by just simulating one periodic domain instead of the entire channel length. This consequently reduces the computational cost dramatically making widespread adaption of CFD-based design method possible.

Thanks to this reduced cost, the SP flow solver finds widespread application in the design of heat exchangers. For example, Ref. [6] uses an SP flow solver to calculate the thermo-hydraulic performance of the off-set strip fins for a wide range of operating conditions. Similarly, Ref. [7] uses a laminar SP flow solver to calculate the performance of wavy fins at different operating conditions. Although the SP flow solver is widely used for the analysis of heat exchangers, some authors also used the method to design heat exchangers. For example, Ref. [8] uses a laminar SP flow solver to solve the flow around offset fins and optimizes the geometry using a gradient-free optimization algorithm. However, the use of adjoint-based shape optimization with an SP flow solver is not reported in the open literature.

Stemming from this shortcoming, the objective of the research reported in this manuscript is to synthesise an adjoint-based shape optimization framework. The framework features a CAD-based geometry parametrization method and a turbulent SP flow solver with isothermal boundaries. The proposed optimization framework is applied to optimize a two-dimensional cylindrical fin. The fin geometry is optimized at two operating conditions, representing laminar and turbulent flow regimes. The problem setup minimizes pressure drop while maintaining the baseline heat-transfer values. The optimization problem was solved using the SNOPT optimizer.

2. Methodology

The proposed optimization framework in this work features five key functional blocks, namely, optimizer, geometry modeler, mesh deformer, flow solver and adjoint solver. The relationship among the different functional blocks in the framework is represented in Figure 1 A block diagram illustrating the proposed optimization framework.Figure 1 below. A brief description of each functional block is elaborated in the following.

1. *Optimizer* The optimizer starts the design process from the baseline design variables α_o and assimilates the objective and constraint values from the flow solver and their corresponding sensitivity from the adjoint solver. Based on the values of the cost functions and their sensitivity the optimizer proposed the next design step with a new design variable α_k. In the current framework SNOPT [9] was used as an optimization algorithm.
2. *Geometry Modeler* The geometry modeler uses a CAD-based curve definition to represent the shape of the fin geometry. The CAD parametrization used in the current study is inherited from Ref. [10], wherein, the shape of the fin is defined using a rib and spar representation to define the control points. Next, the NURBS curve passes through these control points representing the surface of the fin geometry. Thus, the parameters defining the length of the spar, or in other words thickness distribution, define the set of design variables used in the optimization process. Based on the design variables, the geometry modeler provides a surface mesh X_s.
3. *Mesh Deformer* The objective of the mesh deformer is to translate the change in the surface mesh (dictated by the change in the design variables) to the volumetric grid. In the current framework, this process is done using a linear elastic model, wherein, the entire flow domain is represented as an elastic body. The change in the surface geometry is imposed as a Dirichlet boundary on the design surface, thus, giving us the final deformed volumetric grid usually given as X_v.
4. *Flow Solver* The flow around the fin geometry is simulated using the incompressible NS flow solver available within the open-source CFD-solver SU2 [11]. The standard flow solver within SU2 is extended with additional source terms corresponding to those obtained for the SP flow solver with isothermal boundaries. The standard NS equations are represented in their generic form of the equation as

$$\frac{\partial V}{\partial t} + \nabla \cdot F^c(V) + \nabla \cdot F^v(V, \nabla V) + S = 0. \tag{1}$$

In the equation V is the conservative variable, F^c is convective fluxes, F^v is viscous fluxes and S is the volumetric source term. The fluxes and conservative terms remain in their standard form as reported in Ref. [12], where the source term S is given as

$$S = \left(0, -\frac{\Delta p L}{L^2}, (\alpha\lambda_L^2 + u\lambda_L)\theta - 2\alpha\lambda_L\nabla\theta + (-\theta\lambda_L + \nabla\theta)\frac{\nabla\mu_{turb}}{\rho \mathrm{Pr}_{turb}}\right)^{-1} \quad (2)$$

where p is pressure, L is streamwise periodic length, αIs thermal diffusivity, u is velocity, λ_L is exponential, μ is viscosity, ρ is density and Pr is the Prandtl Number. These source terms are the additional terms originating by imposing the periodic assumptions as detailed in Ref. [12]. In this solver, the recovered pressure and temperature are given as

$$p(x) = p(x + L) + \Delta p(x) \quad (3)$$

$$\theta = T_b e^{-\lambda_L x} + C \quad (4)$$

5. *Adjoint Solver* The objective of the adjoint solver is to provide the sensitivity of the objective and the constraints with respect to the design variables. Hence, to achieve this a discrete adjoint approach is employed to differentiate the flow solver. The adjoint equations are derived following the Lagrangian approach elaborated in Ref. [13]. The obtained adjoint equations are the same as the ones reported in Ref. [13]. The additional source terms emerging from the streamwise periodic models are registered as dependent variables in the adjoint solver. The final sensitivity of the objective function with the design variable is obtained using the automatic differentiation algorithm CoDiPack [14].

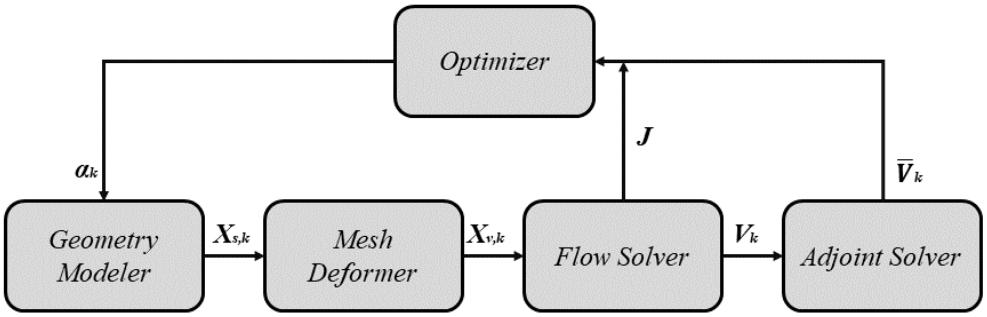

Figure 1 A block diagram illustrating the proposed optimization framework.

3. Test Case

To showcase the capability of the proposed methodology, a two-dimensional section of cylindrical fins was chosen. Such fin configurations are typically used for electronic cooling or as heat exchangers in the oil and gas industry. Figure 2 Illustrates the geometric representation of the used cylindrical fins. The chosen fin configuration features a unitary diameter, and longitudinal and lateral pitches were set to two times the diameter of the cylinder, see Figure 2.

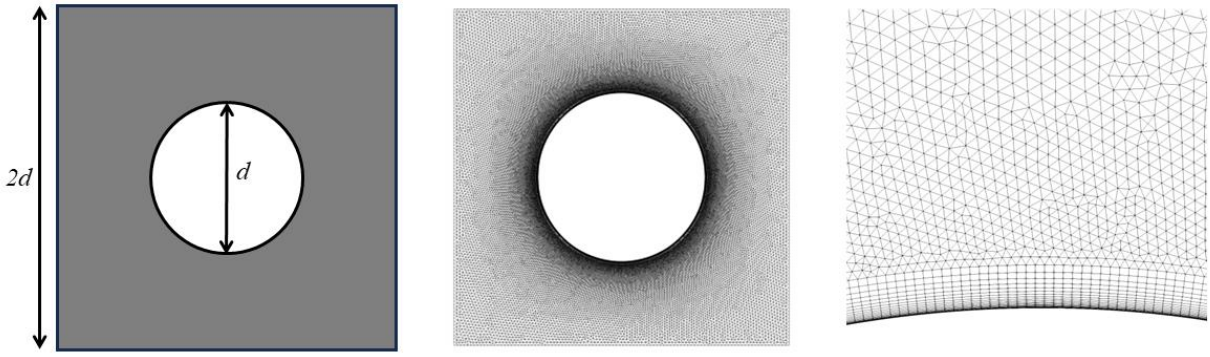

Figure 2: Illustration of used circular fin geometry (left), unstructured mesh used (centre) and boundary layer mesh close to the wall (right)

The selected case was simulated at two operating conditions, namely, laminar, and turbulent, corresponding to a Reynolds number of 132.0 and 132043.3 respectively. In order to achieve the two Reynolds number only the viscosity of the fluid was changed while keeping the rest of the fluid dynamic parameters constant. The flow parameters used to simulate the flow in the heat exchangers are tabulated in Table 1.

Table 1 Parameters based on which the flow simulations were performed for laminar and turbulent flow regimes.

Cases	Re [-]	Velocity [m/s]	Density [kg/m^3]	Diameter [m]	Viscosity [kg/(ms)]
Laminar	132.0	0.285	1.2886	1.0	2.778E-3
Turbulence	132043.3	0.285	1.2886	1.0	2.778E-6

The laminar flow field was simulated using Navier Stokes flow solver, meanwhile, the turbulent flow field was simulated using Reynolds Averaged Navier Stokes (RANS) equations. Both the laminar and the turbulent flow solvers were complemented with their equivalent SP source terms. The convective fluxes were obtained using FDS and second-order accuracy was ensured by using MUSCL flow. The gradients and flow variables needed to evaluate the convective and viscous fluxes were computed using weighted least-squares.

The computational domain was discretized using a hybrid mesh, wherein, quadrilateral elements were clustered close to the wall to ensure a y+ of unity and the rest of the volumetric elements were filled with triangular elements, see Figure 2. The thermodynamic properties were calculated using ideal gas. A converged solution was obtained by using an Euler implicit pseudo time stepping method with a CFL of 40. The mass, momentum and energy equations were converged to six orders of magnitude, which was obtained in 10000 iterations.

4. Results

4.1 Gradient Validation

Before proceeding with numerical optimization, performing is gradient validation study is essential. Such a study assures that the adjoint solvers have sufficiently converged to accurately provide the sensitivity information of the design variables. Figure 3 represents the gradient validation plot obtained for the test case elaborated in this paper. In the plot, the sensitivities obtained from the adjoint solver and that obtained using the first-order accurate finite difference method are plotted against the design variables. It can be observed that the sensitivities obtained using adjoint co-related well with those obtained using finite difference, except for a few design variables. These inaccuracies can be attributed to locations where the flow simulations have not sufficiently converged. Nevertheless, the correlation between the two sensitivities can be deemed sufficient for optimization.

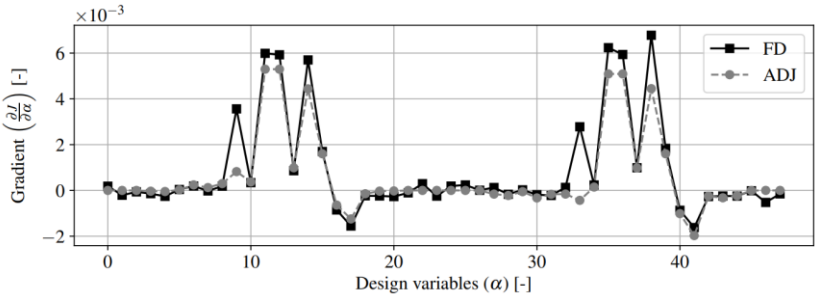

Figure 3 Gradient verification plot of adjoint sensitivities against finite-difference sensitivities.

4.2 Shape optimization

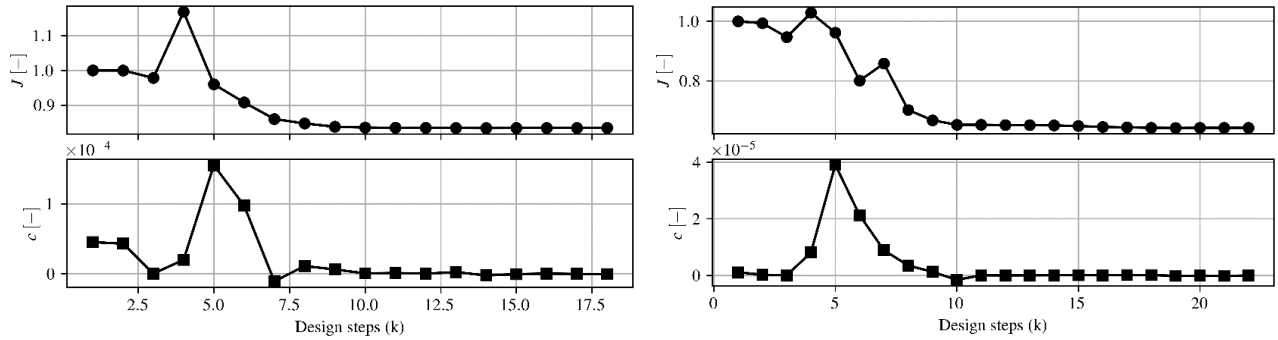

Figure 4 Optimization history circular fins operating laminar (left) and turbulent (right) flow regime.

4.2.1 Laminar Case

The optimization history corresponding to the laminar flow regime is illustrated in Figure 4**Error! Reference source not found.**. It can be observed that the objective function (*J*) was reduced by approximately ~16.5% while satisfying the constraints. Figure 6 (left) illustrates the fin profiles in the baseline and the optimum configurations. It can be observed that the optimised fin features broad leading and trailing edges (between *x* of ±0.6 and ±0.4) as compared to the baseline shape. In addition, the lateral surfaces of optimized fins feature a wavey pattern (between *y* of 0.4-0.5) leading to a higher surface area for heat transfer.

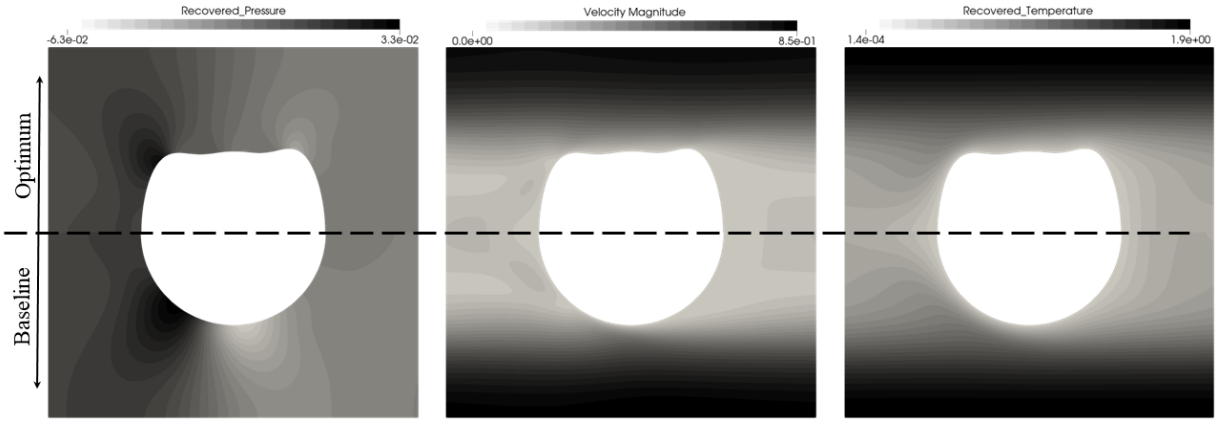

Figure 5 Contour illustrating the contours in the optimum (top) and the baseline (bottom) geometry obtained for the laminar case, the properties represented are recovered pressure (left), velocity magnitude (centre) and recovered temperature (right).

Figure 5 illustrates the contour plots of the flow field around the baseline (bottom) and the optimum (top) geometry obtained using CFD. In the contour plot of recovered pressure (left), it can be observed that the baseline design features a sharp change in the recovered pressure values as compared to that in optimum geometry. Meanwhile, the distribution of velocity magnitude (centre) looks almost identical between the two designs with small changes close to the leading edge and wake. Similarly, reduced temperature (right) seems identical with small variations in leading and trailing edge.

To understand the flow around the fins better, flow properties are plotted along the surface of the fins and are illustrated in Figure 6. It can be observed that the reduced pressure values vary dramatically for the baseline case between *x* of 0.3 to -0.3. This leads to acceleration of the flow close to the wall, consequently leading to high viscous losses. In contrast, it can be observed that the pressure for the optimum geometry reduces gradually in steps, thus leading to a better pressure-drop value over the fins. Meanwhile, the heat-flux distribution over fin surfaces is dramatically different, see Figure 6 (right), the integrated values remain higher for optimum geometry than the baseline. More specifically, the heat rejected by the baseline geometry is 117.3 kW and that of the optimum geometry is 141.3 kW.

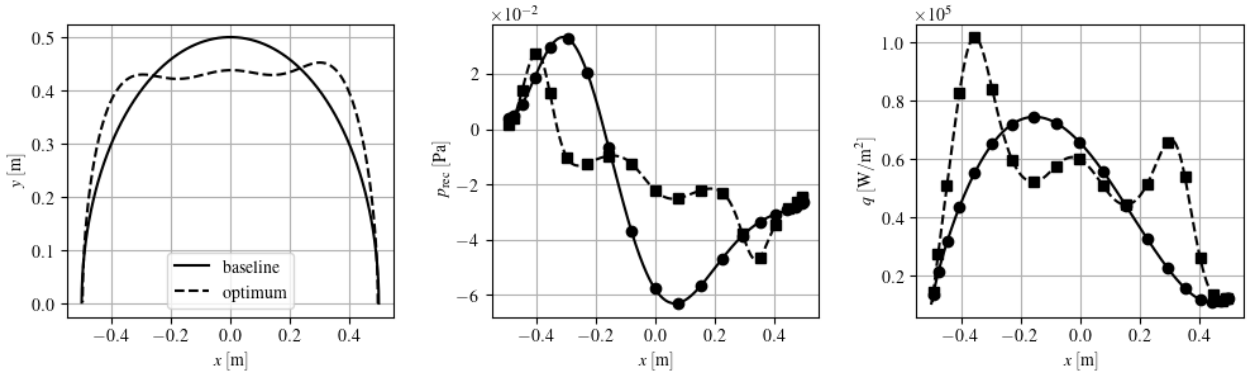

Figure 6 Surface plot along the chord of the fins geometry for laminar case (left) fin profiles (centre) reduced pressure (right) heat flux.

4.2.2 Turbulent Case

Figure 4 Optimization history circular fins operating laminar (left) and turbulent (right) flow regime.(right) illustrates the optimization history plot for the turbulent flow case. It can be observed that the objective of the optimization problem was reduced by 35.8% while the constraint values for the problem were maintained at their baseline value.

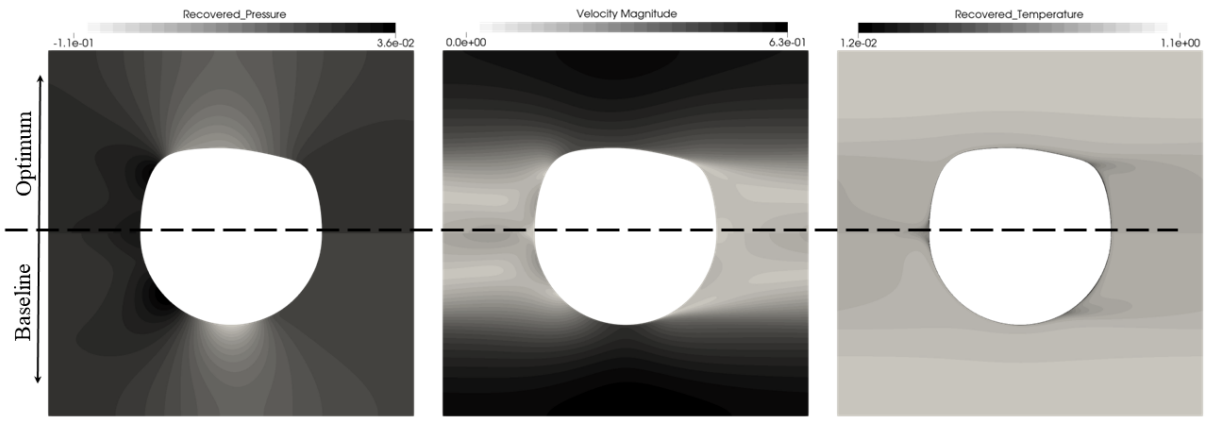

Figure 7 Contour illustrating the contours in the optimum (top) and the baseline (bottom) geometry obtained for the turbulent case, the properties represented are recovered pressure (left), velocity magnitude (centre) and recovered temperature (right).

Figure 8 (left) illustrates the difference between the fin geometry of the baseline and the optimum geometry. It can be observed that the optimum geometry features a blunt leading and trailing edge whereas features a slender overall profile as compared to the baseline geometry. The contour plot of the flow around the baseline and the optimum geometry is illustrated in Figure 7, the top represents the optimum geometry whereas the bottom represents the baseline geometry. It can be observed that the recovered pressure values peak for the baseline case whereas for the optimum geometry, they remain moderate. Similarly, the velocity magnitudes are high for baseline geometry as compared to the optimum geometry. This is because the optimum geometry features a slender fin profile. Meanwhile, the recovered temperature profiles remain almost identical as intended by the imposed constraint on the exponential temperature coefficient.

Figure 8 illustrates the variation of recovered pressure and heat flux along the surface of the fins. It can be observed that the baseline geometry features strong variation in the reduced pressure values as compared to the optimum geometry, between x of -0.4-0.0. As highlighted before, this in turn leads to high viscous losses. Meanwhile, the heat-flux value over the fin surface features dramatically different profiles, however, leading to similar integrated values. More specifically, 5.18 W for baseline and 5.22 W for optimum geometry.

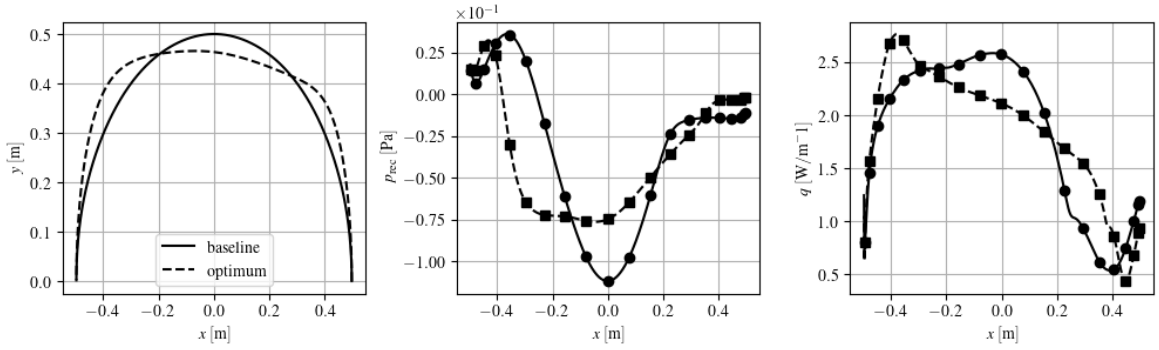

Figure 8 Surface plot along the chord of the fins geometry for turbulent case (left) fin profiles (centre) reduced pressure (right) heat flux.

5. Conclusion

The objective of the manuscript was to propose an adjoint-based optimization framework tailored for heat-exchanger designs featuring a streamwise periodic flow solver. To achieve this, a Python framework using a CAD-based parametrization tool and open-source CFD code SU2 was synthesised. The proposed framework was applied to design inline fin-geometries at two operating conditions, representing laminar and turbulent flow regimes. The results obtained

showcase that the sensitivity obtained using the adjoint-based framework correlates well with the values obtained using the first-order accurate finite difference method. Thus, advocating accurate implementation of the adjoint solver. In addition, the results obtained using the optimization setup show that pressure drop values in the laminar case were improved by 16.9% as compared to its baseline values. Furthermore, for the turbulent case, the pressure drop values were improved by 35.8% while satisfying the imposed constraints.

Future work will focus on extending this work to three-dimensional problems, which will allow the framework to be applied to real-world design problems.

Acknowledgements

Research reported in this manuscript was funded by the Vlaanderen Agentschap Innoveren and Ondernemen (VLAIO), Belgium, through the project IAMHEX (grant number HBC.2021.0801). The computational resources and services used in this work were provided by the HPC core facility CalcUA of the Universiteit Antwerpen, and VSC (Flemish Supercomputer Center), funded by the Research Foundation - Flanders (FWO) and the Flemish Government.

References

[1] D. Bacellar, Z. H. V. Aute and R. Radermacher, "Design optimization and validation of high-performance heat exchangers using approximation assisted optimization and additive manufacturing.," *Science and Technology Build Environment,* pp. 896-911, 2017.

[2] Y. Ge, Y. Lin, S. Tao, Q. He, B. Chen and S.-M. Huang, "Shape optimization for a tube bank based on the numerical simulation and multi-objective genetic algorithm.," *International Journal of Thermal Sciences,* vol. 161, no. 1290-0729, p. 106787, 2021.

[3] T. D. Economon, "Simulation and Adjoint-based design for variable density incompressible flow with heat transfer," in *Multidisciplinary Analysis and Optimization Conference,* Atlanta, Georgia, USA., 2018.

[4] P. P. Raikar, O. Bociar and N. Anand, "Shape and layout optimization of bare-tube heat exchangers using the adjoint method and CAD-based parametrization," in *9th International Conference on Experimental and Numerical Flow and Heat Transfer*, London, UK., 2024.

[5] P. P. Raikar, N. Anand, M. Pini and C. d. Servi, "Concurrent optimization of multiple heat transfer surfaces using adjoint-based optimization with a CAD-based parametrization.," *International Journal of Heat and Mass Transfer,* 2024.

[6] A. Vangeffelen, G. Buckinx, M. R. Vetrano and M. Baelmans, "Friction factor for steady periodically developed flow in micro- and mini-channels with arrays of offset strip fins," *Physics of Fluids,* 2021.

[7] E. Stalio and M. Piller, "Direct numerical simulation of heat transfer in converging-diverging wavy channels.," *Journal of Heat Transfer,* vol. 129, pp. 769-777, 2007.

[8] P. Ranut, G. Janiga, E. Nobile and D. Thevenin, "Multi-objective shape optimization of a tube bundle in cross-flow," *International Journal of Heat and Mass Transfer,* vol. 68, pp. 585-598, 2014.

[9] P. Gill, W. Murray and M. Saunders, "SNOPT: An SQP Algorithm for large-scale constrained optimization.," *SIAM Journal on Optimization,* vol. 47, pp. 99--131, 2002.

[10] R. Agromayor, N. Anand, J.-D. Muller, M. Pini and L. O. Nord, "A Unified geometry parametrization method for turbomachinery blades," *Computer-Aided Design Journal,* vol. 133, p. 102987, 2021.

[11] T. A. Albring, M. Sagebaum and N. R. Gauger, "Efficient Aerodynamics design using the discrete adjoint method in SU2," in *17th AIAA/ISSMO Multidisciplinary Analysis and Optimization Conference,* Washington DC, USA, 2016.

[12] N. Anand, P. P. Raikar and C. d. Servi, “Streamwise periodic, turbulent flow solver for iso-thermal boundary conditions.,” *Under Review,* 2025.

[13] O. Burghardt, P. Gomes, T. Kattmann, T. Economon, N. R. Gauger and R. Palacios, “Discrete adjoint methodology for general multiphysics problems: A modular and efficient algorithmic outline with implementation in an open-source simulation software.,” *Structure and multidisciplinary optimization,* vol. 65, 2022.

[14] M. Sagebaum, T. Albring and N. R. Gauger, “High-performance derivative computation using CoDiPack,” *ACM Transactions on Mathematical Software,* vol. 45, p. 4, 2019.